



Research Article

PROBING MOLECULAR LEVEL INTERACTION OF ANTIFUNGAL DRUGS WITH MODEL MEMBRANES BY MOLECULAR MODELING, MULTINUCLEAR NMR AND DSC METHODS

BHAKTI PAWAR¹, MEENA A. KANYALKAR¹, R. PISSURLENKAR³, MAMATA JOSHI², EVANS C. COUTINHO³ AND SUDHA SRIVASTAVA^{2*}¹ Prin K M Kundnani College of Pharmacy, Cuffe Parade, Mumbai-400005, India, ² National Facility for High Field NMR, Tata Institute of Fundamental Research, Homi Bhabha Road, Mumbai-400005, India. ³ Bombay College of Pharmacy, Kalina, Mumbai-400098, India.

Email: sudha@tifr.res.in

Received 14 Jan 2010, Revised and Accepted 08 Feb 2010

ABSTRACT

In recent years, fungal infections have emerged as a major cause of disease and mortality. Fluconazole and ketoconazole belong to the azole class of antifungal agents. Both act by inhibiting the enzyme lanosterol 14 α -demethylase in fungi, thereby limiting the biosynthesis of ergosterol. Ketoconazole is used to treat mucosal and cutaneous infections caused by *Candida* species and dermatophytosis caused by *epidermophyton*, *trichosporon* and *microsporum* species. Like ketoconazole, fluconazole has been found to be safe and effective in treating infections caused by *Candida* species, however, it is often preferred due to its lesser toxicity, higher potency and greater efficacy. Its favorable attributes, makes it one of the most extensively used antifungal agents and this has resulted in the emergence of resistant fungi strains. Modifications in the structure of fluconazole to circumvent the resistant problems, needs a basic understanding of the mechanism of action of this drug, the interaction of the drug with the fungal membranes. Model membranes prepared from DPPC are good models to probe the mechanism of action of antifungal agents. In view of this, we have studied the interaction of fluconazole and ketoconazole with model membranes prepared from DPPC using multinuclear NMR and DSC techniques. The studies reveal that ketoconazole and fluconazole behave differently in imparting fluidity, dynamics and stability to model membrane. The differences in the effects of these drugs on lipid membranes may be responsible for the differences in their *in vivo* potency.

Keywords: Antifungal; Ketoconazole, Fluconazole; Model membranes; Molecular modelling; NMR; Differential Scanning Calorimeter.

INTRODUCTION

Since 1970s, there has been a steady increase in the incidence of secondary systemic fungal infections. One of the factors aiding the spread of fungal disease is the widespread use of broad-spectrum antibiotics which eliminate or decrease the non-pathogenic bacterial populations that normally compete with fungi. Another is the increased number of individuals with reduced immune responses caused by the acquired immunodeficiency syndrome (AIDS) or by the action of immunosuppressant drugs or cancer chemotherapeutic agents. These factors have contributed to an increase in the prevalence of opportunistic infections, *i.e.* infections with fungi that rarely cause disease in healthy individuals¹.

There are four major families of antifungal agents: the azoles, polyenes, allylamines and echinocandins.

The azole class of compounds is the most popular among the antifungal classes because of its lower toxicity, higher efficacy and a broad spectrum of activity. The main drugs in this class are ketoconazole, fluconazole, itraconazole, miconazole, econazole and voriconazole. These molecules inhibit the fungal cytochrome P450-3A enzyme lanosterol 14 α -demethylase, which is responsible for converting lanosterol to ergosterol the main sterol in the fungal cell membrane. The resultant depletion of ergosterol alters the fluidity of the membrane and this interferes with the replicative process². Azoles also inhibit the transformation of *Candida* yeast cells into hyphae, the invasive and pathogenic form of the parasite.

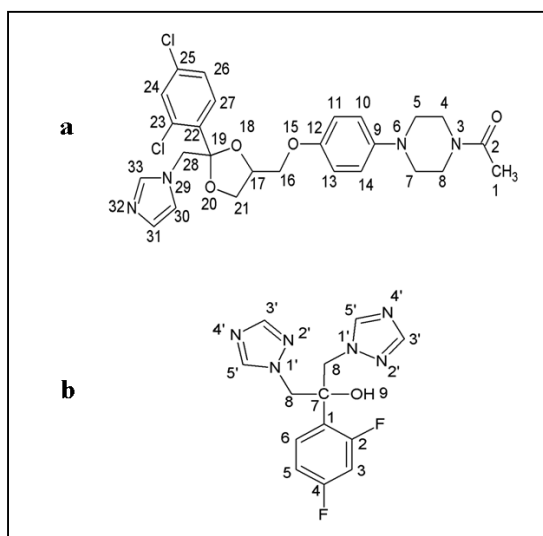


Fig. 1: Molecular structure of (A) Ketoconazole, (B) Fluconazole

Ketoconazole (Fig. 1a) is broad spectrum antifungal agent used both orally and topically to treat mucosal and cutaneous infections caused by *Candida* species and the dermatophytoses caused by *epidermophyton*, *trichosporon*, and *microsporium* species³. It has significant binding to serum proteins. Fluconazole (Fig. 1b) on the other hand is highly active against a variety of fungal pathogens that cause systemic mycoses. Fluconazole is 5–20 fold more active against systemic aspergillosis and against systemic, intracranial and pulmonary cryptococcosis when compared with orally administered ketoconazole⁴. It differs pharmacologically from ketoconazole in that it is highly water soluble, penetrates well into cerebro spinal fluid, has a longer half life, is weakly bound to serum proteins, and is evenly distributed throughout body fluids and tissues⁵. It is relatively safe and effective in treating superficial and systemic infections with *candida* species and as a maintenance therapy for cryptococcal meningitis, particularly in patients with AIDS⁶. Recently it has been reported that extensive use of fluconazole leads to the development of resistant fungi strains.

The differences in the properties and potency of these drugs prompted us to investigate the underlying causes of these differences. A basic understanding of the interaction of these molecules with the fungal membrane is crucial to derive an insight into their mechanism of action⁸. Studies with model membranes can provide an understanding of the transport of the drug inside the fungal cell as well as on its mode of interaction with the fungal cell membrane. We have prepared model membranes from DPPC and used NMR and DSC techniques to probe the effects of these drugs on the dynamics and thermotropics of the lipid membrane. These studies show how drug induced changes in membrane fluidity, stability and polymorphism can be related to the potency and susceptibility of the fungi to the drug. This knowledge can be used to design new fungal inhibitors with better efficacy and lower resistance.

EXPERIMENTAL

Materials

Ketoconazole and fluconazole were gift samples from Kemwell Pvt. Ltd. and Cipla Ltd., India, respectively. L- α -dipalmitoyl phosphatidylcholine (DPPC) was purchased from Sigma Chemicals Co., USA. All chemicals were used without further purification.

Sample preparation for NMR and DSC

Multilamellar vesicles (MLV) were prepared by the standard procedure⁹, where the desired quantity of DPPC and drug were dissolved in chloroform. The solvent was evaporated with a stream of nitrogen so as to deposit a lipid film on the inner walls of the container. The last traces of the solvent were removed by vacuum drying for at least 1 hour. The film was hydrated with the required amount of D₂O (pH 7.2), and incubated in a water bath at 50°C with repeated vortexing. The lipid concentration was maintained at 100 mM for the NMR and 50mM for the DSC experiments. The drug concentrations were varied from 20 mM to 100 mM in the NMR experiments and from 10 mM to 50 mM in the DSC experiments. Unilamellar vesicles (ULV) were prepared by sonicating the dispersions prepared as discussed above using a Branson sonicator-450 with 50% duty cycle, till optical clarity was obtained. NMR spectra of the drugs indicated that these preparations are stable and do not degrade under the experimental conditions.

DSC experiments

DSC experiments were carried out with the differential scanning calorimeter VP-DSC (MicroCal, Northampton MA, USA). The samples were degassed under vacuum before being loaded into the reference and sample cells. A scan rate of 10°C/hr was employed. Data were analyzed with the software ORIGIN provided by MicroCal. All experiments were carried out in the temperature range 20°C to 60°C. Repeated scans for the same sample were generally superimposable.

NMR experiments

NMR experiments were recorded on a BRUKER AVANCE 500 MHz spectrometer. 2D-COSY, NOESY and ROESY experiments were

recorded with the standard pulse sequences¹⁰⁻¹². ³¹P and ¹³C NMR experiments were carried out with a relaxation delay of 1 sec and broadband proton decoupling. The NMR data was processed with Topspin 2.1.

Computational studies

The computational studies were carried out on a CentOS 4.8 Linux workstation with 3GB physical memory and a dual core AMD processor. The construction of the bilayer membrane and the MD simulation studies were carried out in *Desmond* 2.2 (DE Shaw Research, NY)^{13, 14, 15}. The molecular energies in the MD trajectory were analyzed with the molecular dynamics scripts of Desmond Simulation Event Analysis.

Lipid bilayers were constructed from 20 DPPC molecules and 645 solvent molecules. Fluconazole was inserted into the lipid bilayers and the net charge on the system was set to 0. Periodic boundary conditions were applied for the drug-membrane system with the unit cell as orthorhombic ($x=26.63\text{\AA}$, $y=24.47\text{\AA}$, $z=66.71\text{\AA}$). The corresponding system for ketoconazole consisted of a total of 16 lipid molecules and 711 solvent molecules contained within an orthorhombic unit cell of dimensions $x=25.85\text{\AA}$, $y=27.64\text{\AA}$, $z=66.71\text{\AA}$.

To begin with, the drug-bilayer system was relaxed for 0.5 ns by application of semi-isotropic constraints on the system being simulated with the NPT *ensemble* (the temperature and pressure set to 323K and 1.01325 bar respectively). During the initial relaxation period, the drug was restrained in space and only the lipid and solvent molecules were allowed to relax; subsequently the entire drug-lipid complex was allowed to relax. This initial simulation was followed by a 20 ns simulation with snapshots from the trajectory captured every 4.8 ps and the energy recorded every 1.2 ps. Constant temperature and pressure were maintained by coupling to a Berendsen thermostat and barostat.

The electrostatic and van der Waals interactions of the drug with the lipid membrane over the entire trajectory were analyzed with the Desmond Simulation Event Analysis tool.

RESULTS AND DISCUSSION

Molecular Dynamics

To accommodate the drug within the lipid-bilayer system, it was necessary to remove some lipid molecules to make room for the new molecule in the lipid-bilayer. To remove any bad steric contacts between the drug and the lipid-bilayer system, a 0.5 ns MD simulation with the application of semi-isotropic constraints on the unit cell was carried out for an initial relaxation of the drug-lipid complex. After the initial relaxation, the lipid-drug complex was simulated for a period of 20ns to follow the energetics of the interaction.

The simulations indicate that both drugs ketoconazole and fluconazole remain embedded in the hydrophobic region of the lipid-bilayer (Figs. 2a & 2b). Ketoconazole is completely enveloped by the lipid molecules of the bilayer. The dichlorophenyl moiety is in close vicinity of the glycerol and phosphatidyl choline groups while the N-acetylpiperazine phenyl group is seen linearly aligned with the palmitoyl chains of the lipid-bilayer. On the other hand, with fluconazole, the triazole ring is in close vicinity to the ester group made by the palmitoyl moiety with the glycerol backbone. The phenyl ring is lodged in the pocket shaped by the palmitoyl chains of the lipid molecules

The electrostatic and van der Waals interaction energies for ketoconazole and fluconazole with the DPPC molecules, sampled at regular intervals during the simulation and mapped over the entire trajectory are depicted in Figs. 3 and 4 respectively. In case of ketoconazole, the lipid drug complex is more steered towards the van der Waals type of interactions, which seems favorable due to the presence of the rich aromatic system. On the other hand, fluconazole exhibits definite van der Waals interactions with the lipid molecules.

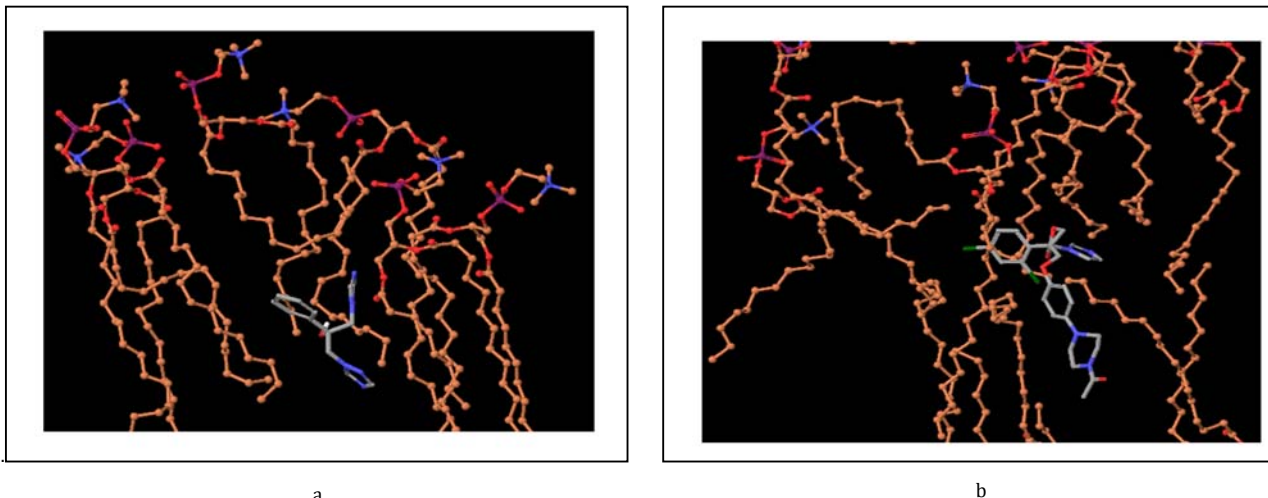


Fig. 2: pictorial representations showing interaction of DPPC molecules with (a) Ketoconazole and (b) Fluconazole

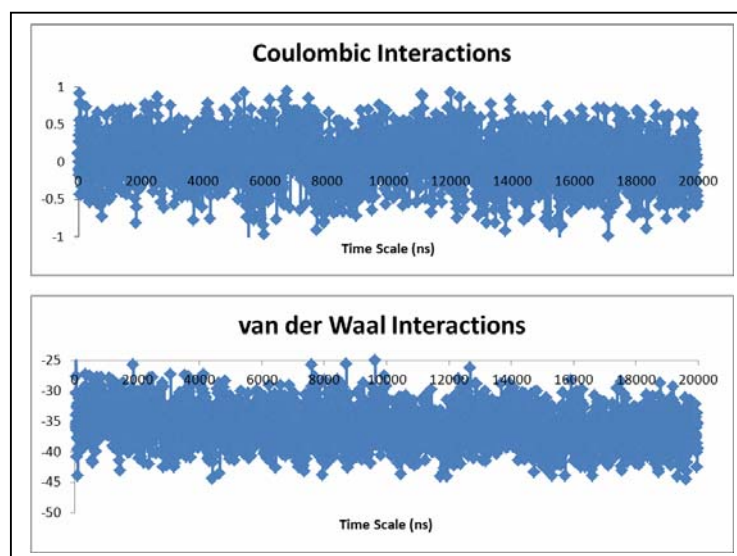


Fig. 3: The variation in the coulombic and van der waals interaction energies in the binding of Ketoconazole with DPPC bilayers

Differential Scanning Calorimetry (DSC)

The thermotropic aspect of the drug-lipid interaction has been studied with DSC by examining the changes in the melting temperature (T_m) of the lipid bilayer and the shape of the DSC trace¹⁶. During heating, the lipid initially undergoes a pretransition ($L_{\beta'} \rightarrow P_{\beta'}$) from an ordered 'gel' state, where the lipids are ordered and tilted ($L_{\beta'}$) to the $P_{\beta'}$ state where the lipids are still ordered and in the gel state but with a minimum in the tilt angle. The pretransition occurs before the main transition and is a small peak compared to the main one. During the main transition ($P_{\beta'} \rightarrow L_{\alpha}$) lipids undergo transition from the ordered state ($P_{\beta'}$) to a 'fluid' disordered state L_{α} ^{17,18}.

Multilamellar bilayers of DPPC alone show a low enthalpy pretransition at 33.7°C arising from the mobility of the polar choline head group of DPPC. In general, pretransition is very sensitive to the presence of impurities and disappears even with small quantities of impurities¹⁹. The main transition peak on the other hand, is observed at 41.3°C and is a consequence of the motions of the alkyl chains of the lipid. The DSC profiles of DPPC incorporated with different concentration of ketoconazole (Fig. 5) give no evidence of

any significant change in the pretransition as well as main transition peaks (Table 1). In sharp contrast, the addition of fluconazole to DPPC bilayers, causes significant changes to the pretransition as well to the main phase transition peaks (T_m) (Fig. 5). Both transition temperatures shift to a lower value and the peaks broaden with increasing concentration of the drug (20mM – 100mM). At a 1:5 fluconazole-DPPC molar ratio, the pretransition temperature shifts to 27.5°C and the main transition to 40.92°C. At 1:2 and 1:1 molar ratios, the pretransition peak is completely abolished and the main transition peak shifts to 39.64°C and 39.43°C respectively. A decrease in the pre-transition and main transition temperatures indicates that fluconazole helps to increase the fluidity of the bilayer. This change in fluidity is a consequence of the increased mobility of both the polar choline head group and in particular the alkyl chains of the lipids. This observation is a logical outcome of the MD simulations where it was seen strong van der Waals interactions causes fluconazole to lodge within the pocket formed by the palmitoyl groups of the lipid tail. There is no evidence of a phase separation or the appearance of any additional endothermic peak which is characteristic of polymorphic phase changes in the bilayer organization of the lipid^{20, 21}. These observations parallel the DSC

study where the presence of cholesterol and peptide was shown to reduce the T_m and stabilize the fluid phase of these membranes²².

The DSC results thus indicate that fluconazole induces significant changes in the physicochemical characteristics of the DPPC bilayers compared to ketoconazole (Table 1).

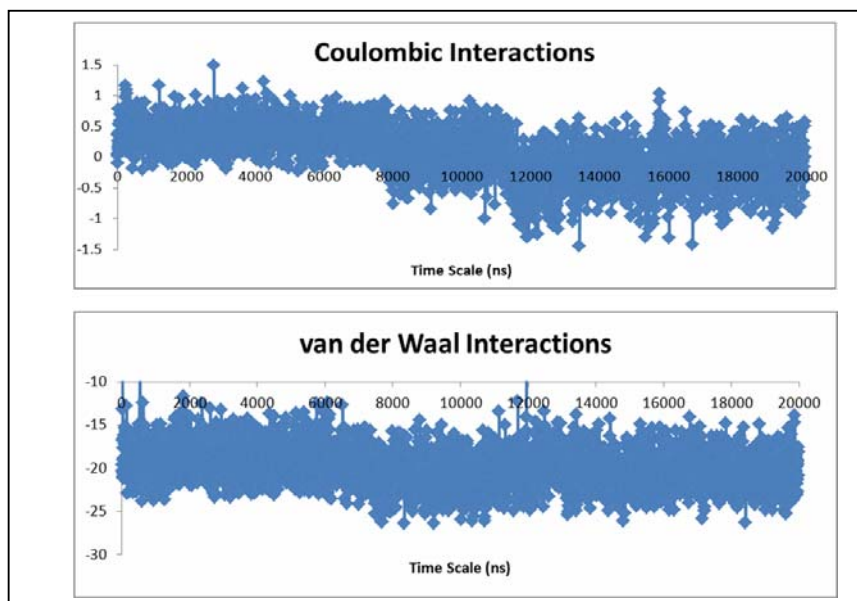


Fig. 4: The variation in the coulombic and van der waals interaction energies in the binding of Fluconazole with DPPC bilayers

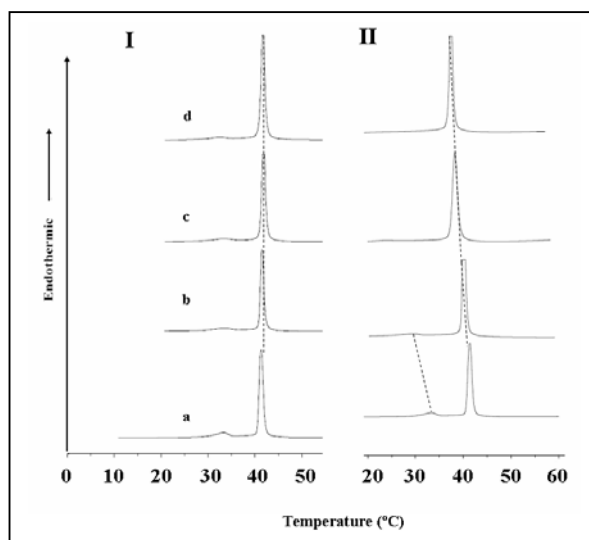


Fig. 5: DSC plots of DPPC (50mm) incorporated with (i) Ketoconazole and (ii) Fluconazole. The drug:lipid molar ratios are (a) 0:100 (b) 1:5 (c) 1:2 (d) 1:1.

Table 1: DSC studies showing the pre-transition and main transition temperatures values of DPPC (50 MM) with varying Ketoconazole and Fluconazole molar ratios

Drug:DPPC	Pretransition		Main transition (t_m)	
	Ketoconazole	Fluconazole	Ketoconazole	Fluconazole
0:100	33.74	33.74	41.30	41.30
1:5	33.70	27.50	41.00	40.92
1:2	33.70	Broad	41.00	39.64
1:1	33.70	Broad	41.00	39.43

NMR Experiments

The ^1H NMR spectra of ketoconazole and fluconazole have been assigned using 2D-COSY. The list of chemical shifts is given in Table 2. The ^1H chemical shifts of DPPC in unilamellar vesicles (ULV) do not change when mixed with either ketoconazole or fluconazole. However, some evidence of drug-lipid interaction is seen in the drug resonances which are considerably broadened in presence of the DPPC molecules (figure not shown).

The NOEs in the 2D-NOESY spectra of ketoconazole (Fig. 6) and fluconazole (Fig. 7) incorporated into ULV provide information on intermolecular interactions between the drug and lipid molecules. The NOEs arise when the two atoms (from same molecule or from two different molecules) are within 5 Å from each other. The NOEs

between the drug and the lipid have been marked out in Figs. 6 and 7. NOEs are observed between the C(17)H, C(5, 7)H₂ of ketoconazole to the methyl group of the fatty acid chain of the lipid; the C(1)H₃, C(5, 7)H₂, C(17)H, C(16, 21)H₂ of ketoconazole show NOEs with the (CH₂)_n group of the lipid chain and C(28)H₂ of ketoconazole shows NOE with $\text{N}(\text{CH}_3)_3$ head group of the lipid. The observed intermolecular NOEs thus indicate that the 1,3-dioxolane ring of ketoconazole binds to the head of lipid bilayer at the lipid water interface. This binding positions the dichlorophenyl moiety in close vicinity of the glycerol substructure and the N-acetyl piperazine phenyl group is then aligned with the palmitoyl chains of the lipid bilayer. Thus the binding of ketoconazole spans the entire length of the lipid molecule from the head group to the hydrophobic interior of the lipid bilayer.

Table 2: ^1H and ^{13}C NMR chemical shifts Δ (PPM) of Ketoconazole and Fluconazole

Ketoconazole in CDCl ₃			Fluconazole in DMSO-D ₆				
Atoms	^1H δ (ppm)	Atoms	^{13}C δ (ppm)	Atoms	^1H δ (ppm)	Atoms	^{13}C δ (ppm)
CH ₃ (1)	2.11	C2	169	CH (8A)	4.57	C2	163.5
CH ₂ (4,8)	3.02	C12	153.2	CH (8B)	4.73	C4	160.5
CH (16)	3.35	C9	145.9	OH (9)	6.50	C3'	151.2
CH ₂ (28)	3.58	C30	138.8	CH (6)	6.85	C5'	145.6
CH ₂ (5,7)	3.73	C23	135.9	CH (5)	7.12	C6	130.1
CH (16)	3.85	C22	134.6	CH (3)	7.17	C1	123.7
CH (17)	4.31	C25	132.9	CH (3')	7.78	C5	111.2
CH (21)	4.40	C24	131.7	CH (5')	8.30	C3	104.1
CH (21)	4.46	C27	129.7			C7	74.2
CH (10,14)	6.76	C32	128.6			C8	55.5
CH (11,13)	6.85	C26	127.5				
CH (27)	6.92	C33	121.3				
CH (31)	7.22	C10,14	119.1				
CH (30)	7.43	C11,13	115.1				
CH (26)	7.47	C19	108.2				
CH (24)	7.53	C17	77				
CH (33)	7.55	C16	74.7				
		C21	67.6				
		C5,28	51				
		C7	46.3				
		C4	41.3				
		C8	29.7				
		C1	21.5				

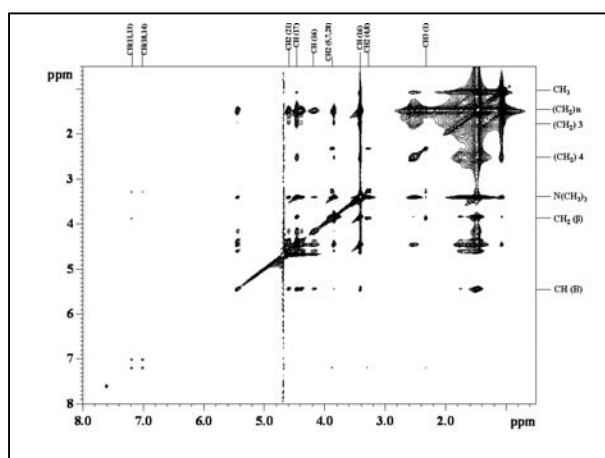


Fig. 6: 500 mhz 2D ^1H noesy spectrum of DPPC unilamellar vesicles incorporated with Ketoconazole (1:2 drug:lipid molar ratio). The experiment was carried out with mixing time of 300 ms and at 323K

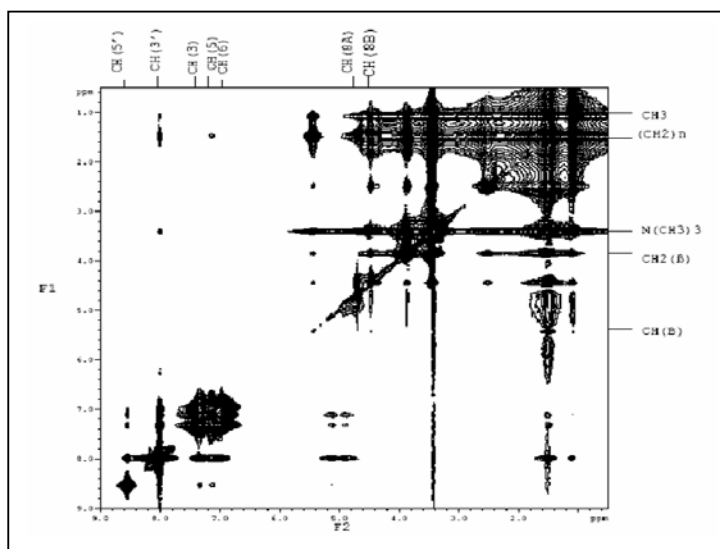


Fig. 7: 500 mhz 2D ^1H noesy spectrum of dppc unilamellar vesicles incorporated with Fluconazole (1:2 DRUG:LIPID MOLAR RATIO). The experiment was carried out with mixing time of 300 ms and at 323K.

In case of fluconazole, the NOEs are as follows: the C(8)H protons of fluconazole show NOE with methyl group of the fatty acid chain of the lipid. Further, the C(8)H, C(3, 5, 6)H and C(3')H protons show NOEs with the $(\text{CH}_2)_n$ group of the lipid chain. Other NOE peaks could not be unambiguously analysed due to spectral overlap. The observed intermolecular NOEs indicate that the aromatic moiety of fluconazole penetrates into the hydrophobic core of the lipid bilayer, binding through hydrophobic interaction. This is exactly in line with the MD simulations and the DSC experiments. The triazole ring of the fluconazole is found to reside at the lipid water interface, showing interactions with the head group of the lipid molecules.

To get further information on the mode of binding, ^{13}C NMR has been carried out for ketoconazole and fluconazole individually and

after incorporation into lipid-bilayers as indicated in Figs. 8 and 9 respectively. The ^{13}C NMR spectrum of DPPC has been assigned using data from literature²³, ketoconazole and fluconazole peaks have been assigned from the DEPT spectra as well as from the multiplicity pattern of the resonances. The ^{13}C chemical shifts of the two drugs are given in Table 2. It is observed that the spectra of both DPPC ULVs and ketoconazole are characterized by sharp resonance lines (Fig. 8a and b). On incorporation of ketoconazole in ULVs, the signals arising from the lipid remain sharp whereas the signals arising from the smaller ketoconazole molecule are broadened significantly (Fig. 8c). This complete broadening of the drug signals indicates that the drug is highly immobilized in the lipid bilayer due to strong hydrophobic interaction.

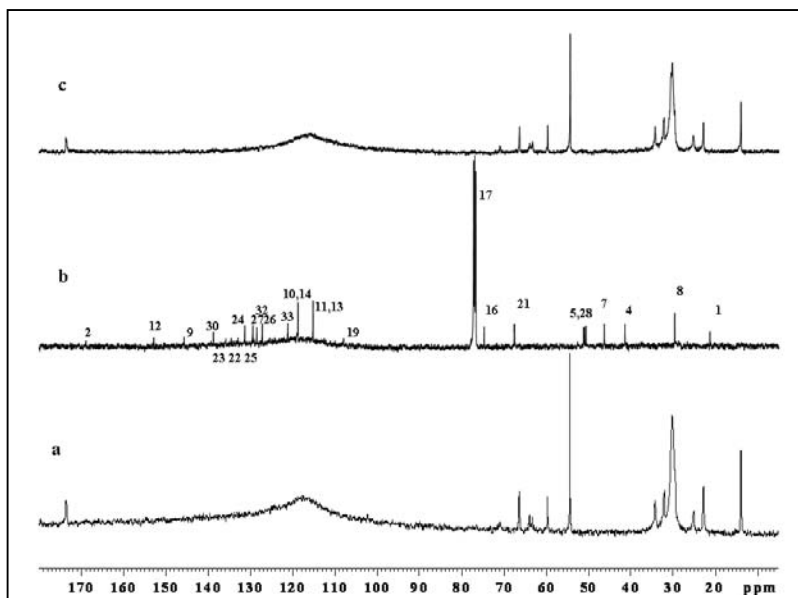


Fig. 8: 125.7 mhz ^{13}C NMR spectra at 323K (A) DPPC unilamellar vesicles (100 mM) (b) Ketoconazole (100 mM) and (c) DPPC unilamellar vesicles incorporated with Ketoconazole (1:2 drug:lipid molar ratio).

The broadening of the drug signals makes it difficult to measure the spin lattice relaxation time (T_1) and spin-spin relaxation time (T_2) which is measure of the overall tumbling and segmental motion of

the molecule. In the fast tumbling range, both T_1 and T_2 are large, of the order of few seconds. Estimates of the spin-spin relaxation times (T_2) from the line widths indicate that T_2 values are about 100ms.

The lower T_2 values indicate that ketoconazole has lost its motional freedom on account of strong binding to the lipid bilayers. The results from ^1H NMR studies corroborate this view (figure not shown). The ^{13}C

chemical shifts and line widths and the pattern of NOEs indicate that ketoconazole gets localized in the hydrophobic core of the lipid-bilayer but does not alter the overall organization of the bilayers.

Table 3: ^{13}C chemical shifts Δ (PPM) of Fluconazole in CDCl_3 and incorporated in dppc vesicles in 1:2 drug:lipid molar ratio at 303 K. $\Delta\delta$ (PPM) shows difference in chemical shifts in two cases

Atoms	δ (PPM)	In lipid vesicles δ (PPM)	$\Delta\delta$ (PPM)
C2	163.5	162.4 (Broad)	1.1
C4	160.5	158.3 (Broad)	2.2
C3'	151.2	151 (Broad)	0.2
C5'	145.6	145.6 (Broad)	-
C6	130.1	Broad beyond detection	-
C1	123.7	Broad beyond detection	-
C5	111.2	111.6 (Broad)	0.4
C3	104.1	Broad beyond detection	-
C7	74.2	74.8 (Broad)	0.6
C8	55.5	55.5 (Broad)	-

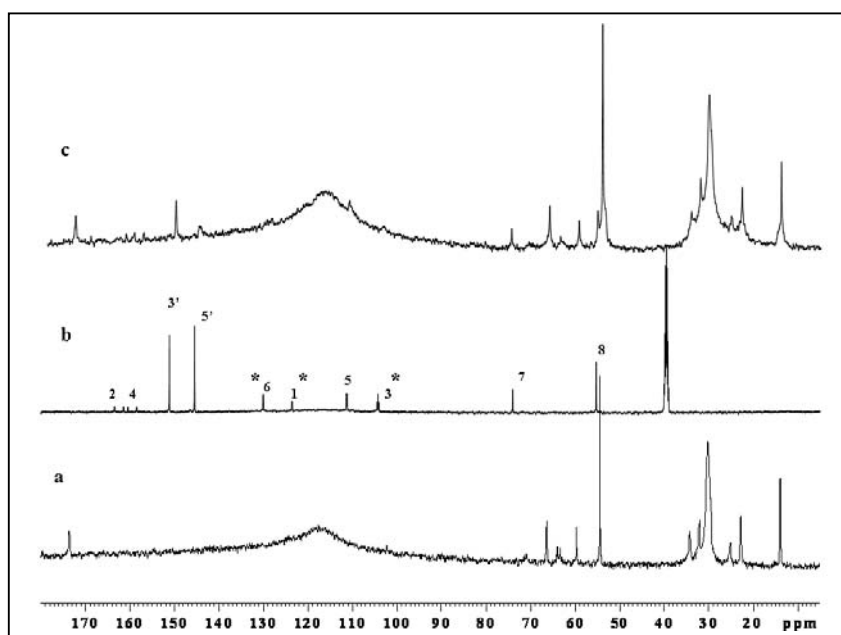


Fig. 9: 125.7 mhz ^{13}C NMR spectra at 323K (A) DPPC unilamellar vesicles (100 mM) (B) Fluconazole (100 mM) and (C) DPPC unilamellar vesicles incorporated with fluconazole (1:2 drug:lipid molar ratio). asterisk (*) indicate signals of fluconazole which are broad and beyond detection on incorporation into DPPC vesicles.

On the other hand, the ^{13}C chemical shifts and line widths of fluconazole incorporated into DPPC ULVs, undergo dramatic changes (Fig. 9). The changes in the chemical shifts and line-widths can be put into three categories: signals that remain sharp but are shifted; those that are broad and shifted and finally those that are broad beyond detection (Table 3). This differential broadening of fluconazole resonances arises because different segments of the drug bind to the lipid-bilayer with different affinities. The differential chemical shift changes and line-widths could also be a result of a slow exchange between bound and free forms of the drug. This means that fluconazole compared to ketoconazole is in a relatively more fluid environment being less tightly bound, and shuttles between bound and free forms.

The ^{31}P NMR resonance line shape is determined by the chemical shift anisotropy (CSA) of the phosphate group coupled with the molecular motions near the head groups²⁴. Line shape characteristics are also indicative of the polymorphism of lipids in model membranes²⁵. In a randomly oriented sample such as DPPC

dispersions in the gel phase, the overall rotational rate is slow. Therefore, one observes a sharp signal at -20 ppm which is indicative of lipid molecules with their long axis oriented parallel to the direction of the magnetic field while for those aligned orthogonal to the field a broad shoulder is seen at 25 ppm. A relatively small sharp peak is seen at 0 ppm from the miniscule population of unilamellar vesicles of small size with fast internal and tumbling motions.

The effect of ketoconazole and fluconazole on the ^{31}P NMR line shape of DPPC vesicles has been followed as a function of both drug concentration (Fig. 10) and temperature (Fig. 11). Increasing concentrations of ketoconazole do not affect the ^{31}P line shape. The bilayer character as seen in the ^{31}P line shape is retained, in other words ketoconazole does not alter the organization of the lipid-bilayers. Increasing concentrations of fluconazole, on the other hand, raises the population of the small unilamellar vesicles as witnessed by the slight increase in intensity of the narrow signal at 0 ppm²⁶. It also perturbs the overall ^{31}P line shape. The sharp signal

at -20 ppm which is indicative of lipid molecules with their long axis oriented parallel to the direction of the magnetic field broadens considerably indicating an increase in the dynamics of this component of the bilayer due to drug binding⁸.

Similar experiments performed as a function of temperature indicate that the drug ketoconazole does alter the intrinsic fluidity of the lipid bilayer and binds through hydrophobic interactions such

that the bilayer character is retained at all temperatures. In contrast, for fluconazole as the temperature increases, the signal sharpens initially until a temperature of 323K is reached. This is followed by a consistent increase in the ³¹P line width with further increase in the temperature. Thus with increasing temperature as more and more drug molecules get bound to the lipid, the fluidity of the bilayer increases and the ³¹P line broadens.

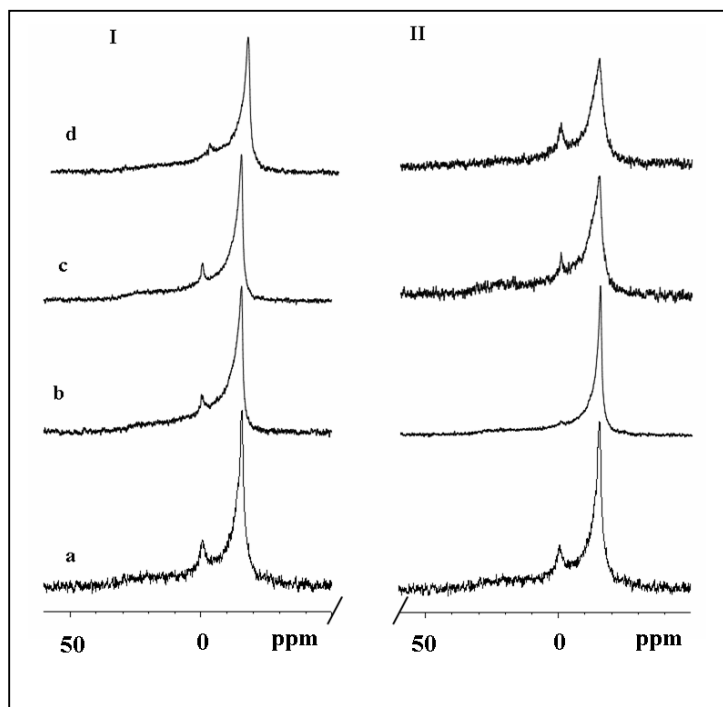


Fig. 10: 202.4 mhz ³¹P NMR spectra of DPPC (100 mm) incorporated with different concentrations of (I) Ketoconazole, (II) Fluconazole drug:lipid molar ratios are a) 0:100 b) 1:5 c) 1:2 and d) 1:1. all spectra have been recorded at 323K.

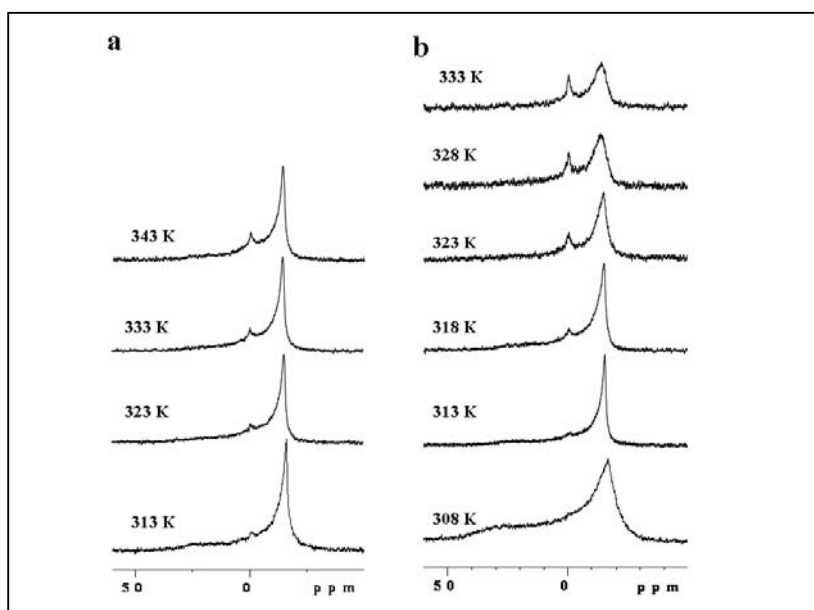


Fig. 11: 202.4 mhz ³¹P NMR spectra of DPPC incorporated with (A) Ketoconazole and (B) Fluconazole, as a function of temperature. drug:lipid molar ratio used are 1:2.

The Chemical shift anisotropy (CSA) can be measured from the low and high field (σ_{\perp} and σ_{\parallel}) shoulder of the spectrum. Figure 12 shows changes in the CSA of the lipid bilayer with increasing concentration of ketoconazole and fluconazole. It is observed that increasing concentration of the two drugs (1:5 to 1:1 drug:lipid molar ratios) causes a decrease in the CSA parameter. Similar changes in CSA are observed with increase in temperature for a fixed drug:lipid molar ratio (Figure not shown). A larger change in CSA in case of fluconazole compared to ketoconazole indicates that the two drugs affect the mobility of the bilayer in different ways due

to differences in their nature of binding. *In-vivo* depletion of ergosterol is known to alter the fluidity of the fungal membrane which in turn affects the replicative processes². Therefore, in the present study, the observed increase in the membrane fluidity and decreased CSA in presence of fluconazole may be a supportive factor for inhibition of fungal replication. In view of this fluconazole may be suitably modified to further increase its lipophilicity. This will aid membrane permeability and thereby enhance inhibition of fungal growth.

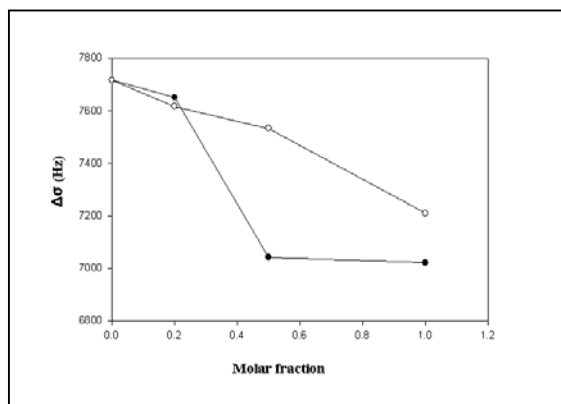


Fig. 12: Change in CSA (Hz) represented by $\Delta\sigma = \sigma_{\perp} - \sigma_{\parallel}$ with increasing drug:lipid molar ratio (O) Ketoconazole and (•) Fluconazole

CONCLUSION

Phospholipids play important roles in biomembranes. They contribute important attributes to the bulk properties and impart specific characteristics to the interactions of biomembranes with drug molecules. It is well known that fluconazole is more potent than ketoconazole. The higher potency of fluconazole may be a result of binding to lipid membranes in the fungal cells that modifies the structural and physicochemical characteristics of the lipid membrane. This spatial proximity of the drug in lipid bilayers changes the fluidity of the membrane by altering the CSA parameter. Such secondary effects may also be responsible for its enhanced *in vivo* potency as an antifungal agent compared to ketoconazole. Moreover, intermolecular interactions seen in the molecular dynamics simulation and supported by NOE data may be helpful in development of new antifungals.

ACKNOWLEDGEMENTS

The authors thank Cipla Ltd. and Kemwell Pvt. Ltd. for the gift sample of fluconazole and ketoconazole respectively. The facilities provided by the National Facility for High Field NMR located at TIFR are gratefully acknowledged. The molecular modeling group is thankful to the Department of Biotechnology (DBT; BT/TF-8/BRB/2009) and the Department of Science and Technology (DST; SR/FST/LSI-163/2003), New Delhi for providing the computational facilities at the Bombay College of Pharmacy.

REFERENCES

- Rang H, Dale M, Ritter J, Flower R: Antibacterial drugs. In Rang & Dale's Pharmacology, Churchill Livingstone, 2007, pp. 844.
- Pereira M, Fachin AL, Martinez-Rossie NM: The gene that determines resistance to tioconazole and to acridine derivatives in *Aspergillus nidulans* may have a corresponding gene in *Trichophyton rubrum*. *Mycopathologia*, 1998; 143:71-75.
- Richardson M, Warnock DW: Fungal Infection: Diagnosis and Management. Wiley-Blackwell, 2008, pp. 1-8.
- Troke PF, Andrews RJ, Marriott MS, Richardson K, Efficacy of fluconazole (UK-49,858) against experimental aspergillosis and cryptococcosis in mice. *Journal of Antimicrobial Chemotherapy*, 1987; 19:663-670.

- Baddley JW and Dismukes WE: Antifungal drugs. In Infectious diseases S. L. Gorbach, J. G. Bartlett, and N. R. Blacklow, editors. Lippincott Williams & Wilkins, Philadelphia. 2004, pp. 317-327.
- Sugar AM and Saunders C: Oral fluconazole as suppressive therapy of disseminated cryptococcosis in patients with acquired immunodeficiency syndrome, *American Journal of Medicine*, 1988;85:481-489.
- Powderly WG, Saag MS, Cloud GA, Robinson P, Meyer RD, Jacobson JM, Graybill JR, Sugar AM, McAuliffe VJ, Follansbee SE: A controlled trial of fluconazole or amphotericin B to prevent relapse of cryptococcal meningitis in patients with the acquired immunodeficiency syndrome, The NIAID AIDS Clinical Trials Group and Mycoses Study Group, *The New England Journal of Medicine*, 1992;326:793-798.
- Srivastava S, Phadke RS, Govil G: Effect of incorporation of drugs, vitamins and peptides on the structure and dynamics of lipid assemblies, *Molecular and Cellular Biochemistry*, 1989;91:99-109.
- Kornberg RD and McConnell HM: Inside-outside transitions of phospholipids in vesicle membranes, *Biochemistry*, 1971;10:1111-1120.
- Aue WP, Bartholdi E, Ernst RR: Two-dimensional spectroscopy. Application to nuclear magnetic resonance, *Journal of Chemical Physics*, 1976;64:2229-2248.
- Jeener J, Meier BH, Bachmann P, Ernst RR: Investigation of exchange processes by two-dimensional NMR spectroscopy, *Journal of Chemical Physics*, 1979;71: 4546-4553.
- Bothner-By AA, Stephens RL, Lee J, Waren CD, and Jeanloz RW: Structure determination of a tetrasaccharide: Transient nuclear Overhauser effects in the rotating frame, *Journal of the American Chemical Society*, 1984;106:811-813.
- Desmond Molecular Dynamics System, version 2.2, D. E. Shaw Research, New York, NY, 2009.
- Maestro-Desmond Interoperability Tools, version 2.2, Schrödinger, New York, NY, 2009.
- Kevin J. Bowers, Edmond Chow, Huafeng Xu, Ron O. Dror, Michael P. Eastwood, Brent A. Gregersen, John L. Klepeis, Istvan Kolossvary, Mark A. Moraes, Federico D. Sacerdoti, John K. Salmon, Yibing Shan, and David E. Shaw, "Scalable Algorithms for Molecular Dynamics Simulations on Commodity Clusters," Proceedings of the ACM/IEEE Conference on Supercomputing (SC06), Tampa, Florida, November 11-17, 2006.

16. Polikandritou Lambros M, Sheu E, Lin JS, Pereira HA, Interaction of a synthetic peptide based on the neutrophil-derived antimicrobial protein CAP37 with dipalmitoylphosphatidylcholine membranes, *Biochim Biophys Acta*, 1997;1329:285-290.
17. Janiak M, Small DM, Shipley GG, Nature of the Thermal pretransition of synthetic phospholipids: dimyristoyl- and dipalmitoyllecithin, *Biochemistry*, 1976;15:4575-4580.
18. Ruocco MJ and Shipley GG: Characterization of the subtransduction of hydrated dipalmitoylphosphatidylcholine bilayers, *Biochimica et Biophysica Acta*, 1982;691:309-320.
19. McElhaney RN: Differential scanning calorimetric studies of lipid-protein interactions in model membrane systems, *Biochim Biophys Acta*, 1986;864:361-421.
20. D'Souza C, Kanyalkar Joshi MM, Coutinho E, Srivastava S: Probing molecularlevel interaction of oseltamivir with H5N1-NA and model membranes by molecular docking, multinuclear NMR and DSC methods, *Biochim. Biophys. Acta*, 2009;1788:484-494.
21. D'Souza C, Kanyalkar Joshi MM, Coutinho E, Srivastava S: Search for novel neuraminidase inhibitors: Design, synthesis and interaction of oseltamivir derivatives with model membrane using docking, NMR and DSC methods, *Biochim. Biophys. Acta*, 2009;1788:1740-1751.
22. Epanand RF, Ramamoorthy A, Epanand RM: Membrane lipid composition and the interaction of pardaxin: the role of cholesterol, *Protein Pept Lett*, 2006;13:1-5.
23. Matsoukas J and Mavromoustakos T: Drug discovery and design: Medical aspects, IOS press, 2002; pp. 129.
24. Srivastava S, Phadke RS, Govil G: Role of tryptophan in inducing polymorphic phase formation in lipid dispersion, *Indiana Journal of Biochemistry & Biophysics*, 1988;25:283-286.
25. Chary KVR and Govil G: NMR in Biological Systems, From Molecules to Humans, Springer, The Netherlands, 2008; pp.291-315.
26. Peuvot J, Schanck A, Deleers M, Brasseur R: Piracetam-induced changes to membrane physical properties, *Biochemical Pharmacology*, 1995;50:1129-1134.